

## Degradation mechanism of Schottky diodes on inductively coupled plasma-etched n-type 4H-SiC

Kyoung Jin Choi, Sang Youn Han, and Jong-Lam Lee

Citation: *Journal of Applied Physics* **94**, 1765 (2003); doi: 10.1063/1.1581347

View online: <http://dx.doi.org/10.1063/1.1581347>

View Table of Contents: <http://scitation.aip.org/content/aip/journal/jap/94/3?ver=pdfcov>

Published by the [AIP Publishing](#)

---

### Articles you may be interested in

[Electrical characterization of \(Ni/Au\)/Al<sub>0.25</sub>Ga<sub>0.75</sub>N/GaN/SiC Schottky barrier diode](#)

*J. Appl. Phys.* **110**, 013701 (2011); 10.1063/1.3600229

[Analysis of surface morphology at leakage current sources of 4H-SiC Schottky barrier diodes](#)

*Appl. Phys. Lett.* **98**, 222111 (2011); 10.1063/1.3597413

[Response to "Comment on 'Interpretation of Fermi level pinning on 4H-SiC using synchrotron photoemission spectroscopy'" \[Appl. Phys. Lett.85, 2661 \(2004\)\]](#)

*Appl. Phys. Lett.* **85**, 2663 (2004); 10.1063/1.1795356

[Low temperature annealing of 4H-SiC Schottky diode edge terminations formed by 30 keV Ar + implantation](#)

*J. Appl. Phys.* **87**, 3973 (2000); 10.1063/1.372443

[Evaluation of damage induced by inductively coupled plasma etching of 6H-SiC using Au Schottky barrier diodes](#)

*Appl. Phys. Lett.* **73**, 653 (1998); 10.1063/1.121937

---

A banner for '2014 Special Topics' with an orange background. The title '2014 Special Topics' is in large white font. Below it are five circular icons representing different material categories: Perovskites (red and black geometric shapes), 2D Materials (red and blue lattice structure), Mesoporous Materials (green and yellow porous structure), Biomaterials/Bioelectronics (yellow and black grid), and Metal-Organic Framework Materials (brown and yellow porous structure). At the bottom left is the 'AIP | APL Materials' logo, and at the bottom right is a red ribbon with the text 'Submit Today!' in white.

2014 Special Topics

PEROVSKITES

2D MATERIALS

MESOPOROUS MATERIALS

BIOMATERIALS/ BIOELECTRONICS

METAL-ORGANIC FRAMEWORK MATERIALS

AIP | APL Materials

Submit Today!

# Degradation mechanism of Schottky diodes on inductively coupled plasma-etched *n*-type 4H-SiC

Kyoung Jin Choi, Sang Youn Han, and Jong-Lam Lee<sup>a)</sup>

*Department of Materials Science and Engineering, Pohang University of Science and Technology (POSTECH), Pohang, Kyungbuk 790-784, Korea*

(Received 18 November 2002; accepted 18 April 2003)

The degradation mechanism of Ta Schottky contact on 4H-SiC exposed to an inductively coupled plasma (ICP) was studied using deep-level transient spectroscopy and angle-resolved x-ray photoelectron spectroscopy (XPS). Four kinds of traps  $T_1$ ,  $T_2$ ,  $T_3$ , and  $T_4$  were observed in the ICP-etched sample. The  $T_4$  trap was deep in the bulk, but the shallower levels,  $T_1$ ,  $T_2$  and  $T_3$ , were localized near the contact. From angle-resolved XPS measurements, the ICP-etched surface was found to be carbon deficient, meaning the production of carbon vacancies by ICP etching. The activation energies 0.48 ( $T_3$  trap) and 0.60 eV ( $T_4$  trap) agreed well with the previously proposed energy level of  $V_C$  (0.5 eV). The ICP-induced traps provided a path for the transport of electrons at the interface of metal with SiC, leading to a reduction of the Schottky barrier height and an increase of the gate leakage current. © 2003 American Institute of Physics. [DOI: 10.1063/1.1581347]

## I. INTRODUCTION

Reactive ion etching (RIE) is commonly used in the fabrication of SiC devices because of the inherent chemical stability of SiC, but it leaves ion damage on the etched surface.<sup>1</sup> Inductively coupled-plasma (ICP) etching has significant advantages over RIE such as little damage on the etched surface due to lower ion energies and higher plasma densities.<sup>2</sup> However, ICP etching still causes degradation of the electrical properties, depending on the type of etch gas and plasma power.<sup>3</sup> The degradation of electrical properties of SiC Schottky contacts on etched surfaces has been attributed to surface contamination resulting from the reaction of the residual etching gas with SiC. A significant amount of chemical bonds associated with etching gas elements was found on the etched surface.<sup>1,4</sup> Another possible origin of the degradation in electrical characteristics could be the generation of microstructural imperfections on the etched surface or carrier traps.<sup>3</sup>

Current-voltage ( $I$ - $V$ ) measurement is a common method for monitoring the effects of dry etching damage of the electrical properties of Schottky diodes, namely, the Schottky barrier height ( $\phi_B$ ), ideality factor ( $\eta$ ) and reverse leakage current ( $I_R$ ). However, it is not improper for the quantitative evaluation of dry-etching-induced traps. Quantitative information on dry-etching-induced traps such as their activation energy, concentration, and depth distribution can be obtained through deep-level transient spectroscopy (DLTS). The depth distribution of deep levels obtained provide critical information for interpreting changes in the electrical properties of devices.<sup>5,6</sup> The dry-etching-induced traps are usually localized near the surface, causing surface band bending below the surface. Surface band bending can be determined by observing the change in binding energy of each element on the surface using x-ray photoemission spectroscopy (XPS) since the binding energy is defined as the difference in energy between a corresponding energy level and the Fermi energy level.<sup>7</sup> Thus, XPS and DLTS measurements should be a complementary tool in studying dry-etching-induced damage. However, no work has been published on the influence of ICP etching on the generation of deep levels in SiC, especially for the surface chemistry of ICP-etched SiC.

In this work, we report on an investigation of the electrical properties of metal contacts on ICP-etched SiC. The surface damage induced by ICP etching was characterized using DLTS. Angle resolved XPS was employed to examine the atomic binding energy and atomic composition of the treated surface. From these, the mechanism of the degradation of Schottky characteristics in Ta/4H-SiC Schottky diodes is proposed.

In this work, we report on an investigation of the electrical properties of metal contacts on ICP-etched SiC. The surface damage induced by ICP etching was characterized using DLTS. Angle resolved XPS was employed to examine the atomic binding energy and atomic composition of the treated surface. From these, the mechanism of the degradation of Schottky characteristics in Ta/4H-SiC Schottky diodes is proposed.

## II. EXPERIMENT

The SiC sample used in this study was a 10- $\mu\text{m}$ -thick *n*-type 4H-SiC epitaxial layer ( $n=4.2\times 10^{15}\text{ cm}^{-3}$ ) grown on a highly doped substrate ( $n=2\times 10^{18}\text{ cm}^{-3}$ ). A 150-nm-thick Ni layer was deposited onto the backside of the samples by electron-beam evaporation, followed by rapid thermal annealing at 950 °C for 90 s to form a backside ohmic contact. The surface was treated with two types of methods prior to deposition of the Schottky metal. One set was prepared by de-oxidizing the sample using a buffered oxide etchant (BOE etched) and the other was etched with ICP for 3 min using three types of gases,  $\text{Cl}_2$ ,  $\text{O}_2$  and  $\text{N}_2$  (ICP etched).

In the ICP treatment, a base pressure of  $5\times 10^{-5}$  Torr and a flow rate of 10 sccm of each etching gas were used. Circular pads with radius of 100  $\mu\text{m}$  were patterned on both samples using image-reversal photolithography. The patterned samples were dipped into BOE for 1 min to remove the native oxides, possibly formed during the ICP treatment,

<sup>a)</sup>Electronic mail: jlllee@postech.edu

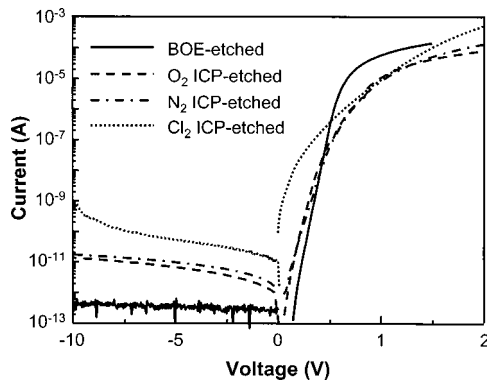


FIG. 1.  $I$ - $V$  characteristics of Ta Schottky diodes fabricated on both BOE- and ICP-etched  $n$ -type 4H-SiC samples.

followed by deposition of a 100-nm-thick Ta Schottky contact by electron-beam evaporation.

The chemical composition and surface band bending at the surface of SiC before and after ICP treatment were characterized using angle-resolved XPS measurements. Si  $2p$ , C  $1s$ , O  $1s$ , and Cl  $2p$  photoemission spectra were recorded with Al  $K\alpha$  radiation (1487.04 eV) operating at 15 kV. In order to obtain depth information on the atomic compositions at the surface of SiC, the take-off angle  $\theta$  between the SiC surface and the trajectory of the emitted electron was changed from  $30^\circ$  to  $90^\circ$ . The smaller the  $\theta$ , the larger the photoelectrons that emit from near the surface region because of the inelastic mean-free path of photoelectrons. The operating pressure was about  $4 \times 10^{-10}$  Torr.

$I$ - $V$  curves were measured to determine the Schottky characteristics, namely,  $\phi_B$ ,  $\eta$  and  $I_R$ . The change in surface morphology caused by ICP etching was monitored using atomic force microscopy (AFM). In the DLTS measurements, the ratio of sampling times  $t_2/t_1$  was kept at 4, with  $t_1$  changed from 50 to 800 ms. In order to investigate the depth distribution of the trap density, the reverse ( $V_m$ ) and the pulse bias ( $V_p$ ), applied to the Schottky contact, were systematically changed in the DLTS measurements.

### III. RESULTS AND DISCUSSION

Figure 1 shows forward and reverse  $I$ - $V$  characteristics of Ta Schottky diodes fabricated on both BOE-etched and ICP-etched samples. Using the thermionic emission model,  $\phi_B$  and  $\eta$  were extracted from the intercept and the slope of the line extrapolated in the semilogarithmic plot of the current density versus forward voltage, summarized in Table I. The  $\phi_B$  decreased by 0.17 and 0.21 eV after ICP etching with  $O_2$  and  $N_2$ , respectively. In the case of ICP etching using  $Cl_2$ , however, the degradation was so severe that the

TABLE I.  $\phi_B$  and  $\eta$  of Ta Schottky contacts on BOE- and ICP-etched SiC.

	BOE etched	ICP etched		
		$O_2$	$N_2$	$Cl_2$
$\phi_B$ (eV)	1.10	0.93	0.89	not measured
$\eta$	1.02	1.17	1.53	not measured

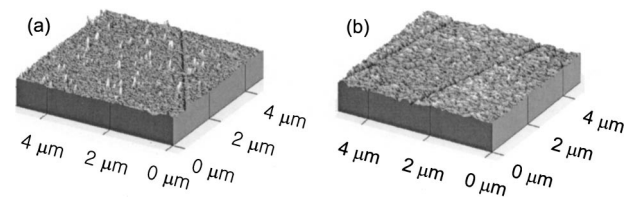


FIG. 2. Three-dimensional AFM images: (a) BOE-etched and (b)  $Cl_2$  ICP-etched SiC samples.

linear region in the forward  $I$ - $V$  curve almost disappeared and thus thermionic emission was not applicable. This suggests that the transport mechanism of electrons at the interface of Ta with SiC can be no longer described in terms of the thermionic emission model.

Figure 2 displays AFM images of both BOE-etched and  $Cl_2$  ICP-etched surfaces. In the BOE-etched sample, a number of protrusions and polishing scratches are clearly visible. In the ICP-etched one, only a small number of protrusions was observed and the roughness was reduced from 12.0 to 7.8 Å. This means that no preferential loss of one element<sup>8</sup> in SiC occurred during ICP etching. This suggests that the degradation in electrical properties by ICP etching is not directly related to the surface morphology.

Figure 3 shows DLTS spectra of Schottky diodes prepared with the surface treatment. No traps were found in the BOE-etched sample, but a broad asymmetric electron-trap signal was observed in the  $Cl_2$  ICP-etched sample. In order to obtain depth information on ICP-induced traps,  $V_p$  and  $V_m$  were simultaneously changed. As the depletion layer width increased deep into the bulk region by changing the bias condition from ( $V_p=1$  V,  $V_m=0$  V) to ( $V_p=0$  V,  $V_m=-1$  V), the peak height of the ICP-induced traps was reduced significantly, and the peak temperature moved a little towards the higher temperature region. When the bias was decreased to below  $-1$  V, the signal completely disappeared. These results suggest that the ICP treatment produced a number of traps near the surface.

The penetration depth of ICP etching damage is estimated from the change in depletion width<sup>9</sup>  $W$  with  $V_m$ :

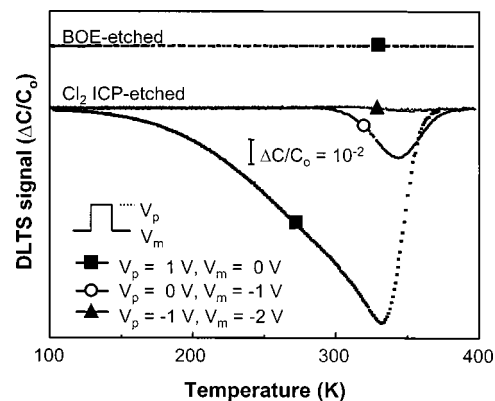


FIG. 3. Capacitance DLTS spectra of Schottky diodes fabricated on both BOE-etched and  $Cl_2$  ICP-etched SiC samples.

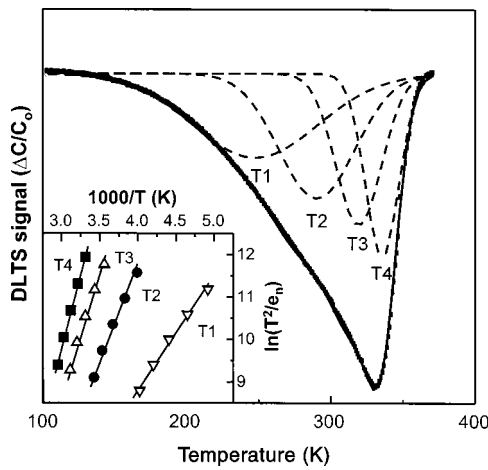


FIG. 4. Separation of a broad electron trap into four discrete traps,  $T_1$ ,  $T_2$ ,  $T_3$ , and  $T_4$ . The inset shows Arrhenius plots for each peak.

$$W = \left( \frac{2\varepsilon_s(V_{bi} - V_m)}{qN_D} \right)^{1/2}, \quad (1)$$

where the built-in potential  $V_{bi} = \phi_B + [kT \ln(N_C/N_D)] - kT$ . Here,  $N_D$  is the donor concentration and  $N_C$  is the effective density of states of the conduction band<sup>10</sup> for 4H-SiC,  $1.66 \times 10^{19} \text{ cm}^{-3}$ . The depletion width was determined to be  $0.36 \mu\text{m}$  at  $V_m = 0 \text{ V}$  and  $0.63 \mu\text{m}$  at  $V_m = -1 \text{ V}$ , respectively. Considering the average ion energy of  $\sim 300 \text{ eV}$ , caused by a chuck power of  $100 \text{ W}$  during ICP etching, the distribution of ICP-induced defects was quite deep and reached  $0.63 \mu\text{m}$ . This suggests that such deep penetration of ICP-induced defects resulted from the channeling of incoming ions. According to molecular dynamics simulations on silicon and III-V compound semiconductors, ion channeling is possible even at extremely low energies.<sup>11,12</sup>

The broad peak observed in the ICP-etched sample was asymmetric as shown in Fig. 3, which means that several kinds of traps are superimposed in the peak. Thus, the broad peak was separated considering that the full width at half maximum of the trap, which was observed at  $V_p = 0 \text{ V}$  and  $V_m = -1 \text{ V}$ , should not be changed by different bias conditions and the number of the separated peaks should be as low as possible with a good fit to the original broad peak. Keeping this in mind, the broad peak separated best into four peaks, namely,  $T_1$ ,  $T_2$ ,  $T_3$ , and  $T_4$ , plotted in Fig. 4. The temperature dependence of each peak is plotted in the inset of Fig. 4. From this,  $E_a$  and  $\sigma_n$  were determined, summarized in Table II. The values of  $E_a$  and  $\sigma_n$  for  $T_4$  are similar to those for the signal observed for the same bias condition

TABLE II.  $E_a$  and  $\sigma_n$  for traps  $T_1$ ,  $T_2$ ,  $T_3$ , and  $T_4$ .

Trap level	$E_a$ (eV)	$\sigma_n$ (cm <sup>2</sup> )
$T_1$	$0.23 \pm 0.03$	$8.42 \times 10^{-21}$
$T_2$	$0.37 \pm 0.01$	$4.24 \times 10^{-19}$
$T_3$	$0.48 \pm 0.02$	$4.36 \times 10^{-18}$
$T_4(V_p = 1 \text{ V}, V_m = 0 \text{ V})$	$0.60 \pm 0.01$	$1.02 \times 10^{-16}$
$T_4(V_p = 0 \text{ V}, V_m = -1 \text{ V})$	$0.70 \pm 0.01$	$2.27 \times 10^{-15}$

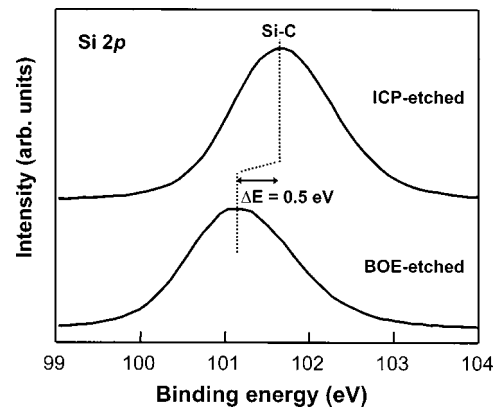


FIG. 5. Change in Si  $2p$  core level XPS spectra with ICP etching. There was no change in the FWHM by ICP etching but the binding energy shifted towards the higher energy region.

( $V_p = 0 \text{ V}, V_m = -1 \text{ V}$ ) as in Fig. 3. This means that these signals originate from the same traps. However, the  $E_a$  for  $T_4$  increased by  $0.1 \text{ eV}$  at the higher reverse bias condition ( $V_p = 0 \text{ V}, V_m = -1 \text{ V}$ ). This can be explained by the Poole-Frenkel effect.<sup>13</sup> The electric field is highest at the interface and then decreases away from the interface. Thus, the  $E_a$  of  $T_4$  near the contact is smaller than that far from the contact.

In order to suggest the origin for the ICP-induced trap, the changes in chemical composition and surface band bending were investigated using angle-resolved XPS measurements. Figure 5 shows Si  $2p$  core level spectra before and after ICP treatment. There was no change in the full width at half maximum (FWHM), but the binding energies of the spectra shifted  $0.5 \text{ eV}$  toward the higher energy region. The binding energy of a XPS spectrum is defined as the difference in energy between the corresponding energy level and the Fermi energy level ( $E_F$ ) at the surface. Therefore, the shift of binding energy toward higher energy region indicates that  $E_F$  at the surface of SiC moved near the conduction band edge by the ICP treatment, resulting in a decrease of the effective  $\phi_B$ , consistent with the result in Fig. 1.

The relative atomic ratio of Si to C atoms, Si/C, the atomic percentage of each element, was determined by integrating intensities of the Si  $2p$ , C  $1s$ , O  $1s$  and Cl  $2p$  core level spectra, summarized in Table III. The ratio of Si/C increased on the ICP-etched surface at all take-off angles. This means that the SiC surface became C deficient and a number of  $V_C$  were produced by ICP etching. In SiC,  $V_C$  was proposed to be a deep donor and the Si vacancy  $V_{Si}$  a deep acceptor.<sup>14,15</sup> The ionization energy level of  $V_C$  is located  $0.5$

TABLE III. Atomic percentage determined by integrating the area of each XPS spectrum and the ratio of Si/C for the BOE- and ICP-etched surfaces with take-off angle  $\theta$ . The values in parentheses were normalized to those of BOE-etched samples for comparison.

	$\theta$ (deg)	Si	C	O	Cl	Si/C
BOE etched	90	37	53	10		0.69 (1)
	(at. %)	30	28	58	14	0.49 (1)
ICP etched	90	43	46	8	3	0.93 (1.34)
	(at. %)	30	35	48	12	5

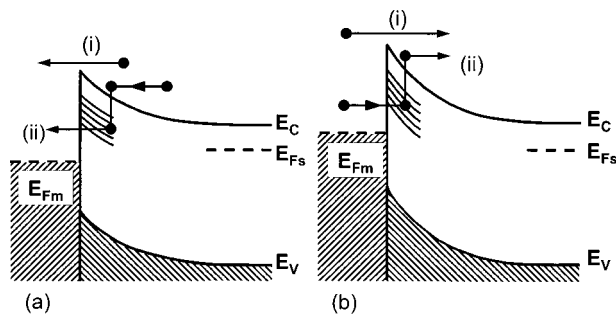


FIG. 6. Schematic of electron transport through ICP-induced traps near the interface of Ta with ICP-etched SiC: (a) under forward bias and (b) under reverse bias conditions.

eV under the conduction band edge.<sup>14</sup> The energy level of  $V_C$  agrees well with the activation energies 0.48 and 0.60 eV of major ICP-induced traps,  $T3$  and  $T4$ , as shown in Fig. 4. Thus, it can be suggested that the origin of the ICP-induced traps is  $V_C$  or  $V_C$ -related complex of point defects.

The electrical degradation of Schottky diodes by ICP etching in Fig. 1 can be explained by the tunneling of electrons via ICP-induced traps at the interface of Ta with SiC. Under a forward bias condition, electrons could be transported across the contact by (i) thermionic emission of electrons over the Schottky barrier and (ii) tunneling of electrons through the ICP-induced traps, shown in Fig. 6(a). The electron transport under a reverse bias condition can also be described in a similar way as shown in Fig. 6(b). The transport of electrons through the ICP-induced traps could be probable because the ICP-induced traps, whose energy levels are close to each other, provide small energy “steps,” which can easily be surmounted by injected electrons.<sup>13</sup> These caused the increase in  $I_R$ , and led to deviation of the forward  $I$ - $V$  characteristics from those described by the thermionic emission model, as shown in Fig. 1.

#### IV. CONCLUSION

Schottky diodes were fabricated on both the BOE- and ICP-etched  $n$ -type 4H-SiC surfaces. The Schottky diode on the ICP-etched surface exhibited severe degradation in

Schottky characteristics, namely, the decrease of  $\phi_B$  and the increase of  $I_R$ . In DLTS measurements of the Schottky diodes on the ICP-etched SiC surface, four kinds of traps,  $T1$ ,  $T2$ ,  $T3$ , and  $T4$ , were found. Trap  $T4$  was deep in the bulk of SiC, but  $T1$ ,  $T2$  and  $T3$  were near the contact. From angle-resolved XPS measurements, the ICP-etched surface was found to be C deficient, meaning the production of  $V_C$  on the surface during the ICP etching. In comparing the activation energy of each trap with the energy level of  $V_C$  ( $\sim 0.5$  eV), the  $T3$  and  $T4$  traps could originate from  $V_C$ . From this, it was suggested that ICP etching produced  $V_C$  or a  $V_C$ -related complex on the surface of  $n$ -type 4H-SiC, causing electrical degradation in the Schottky diode due to the transport of electrons via those interfacial traps.

#### ACKNOWLEDGMENT

This work was performed through the National Research Laboratory project sponsored by the Korea Institute of Science and Technology Evaluation and Planning (KISTEP).

- <sup>1</sup>D. J. Morrison, A. J. Pidduck, V. Moore, P. J. Wilding, K. P. Hilton, M. J. Uren, and C. M. Johnson, *Mater. Sci. Forum* **338–342**, 1199 (2000).
- <sup>2</sup>F. A. Khan, B. Roof, L. Zhou, and I. Adesida, *J. Electron. Mater.* **30**, 212 (2001).
- <sup>3</sup>V. Khemka, T. P. Chow, and J. R. Gutmann, *J. Electron. Mater.* **27**, 1128 (1998).
- <sup>4</sup>B. Li, L. Cao, and J. H. Zhao, *Appl. Phys. Lett.* **73**, 653 (1998).
- <sup>5</sup>K. J. Choi and J.-L. Lee, *IEEE Trans. Electron Devices* **48**, 190 (2001).
- <sup>6</sup>K. J. Choi, J.-L. Lee, and H. M. Yoo, *Appl. Phys. Lett.* **75**, 1580 (1999).
- <sup>7</sup>D. Briggs, *Handbook of X-ray and Ultraviolet Photoelectron Spectroscopy*, (Heyden, London 1978), pp. 121–127.
- <sup>8</sup>C. R. Eddy, Jr. and B. Molnar, *J. Electron. Mater.* **28**, 314 (1999).
- <sup>9</sup>E. H. Rhoderick and R. H. Williams *Metal-Semiconductor Contacts* (Clarendon, Oxford 1988), pp. 38–41.
- <sup>10</sup>M. Bakowski, U. Gustavsson, and U. Lindefelt, *Phys. Status Solidi A* **162**, 421 (1997).
- <sup>11</sup>N. G. Stoffel, *J. Vac. Sci. Technol. B* **10**, 651 (1992).
- <sup>12</sup>A. Boussetta, J. A. van den Berg, R. Valizedah, D. G. Armour, and P. C. Zalm, *Nucl. Instrum. Methods Phys. Res. B* **55**, 565 (1991).
- <sup>13</sup>P. A. Martin, B. G. Streetman, and K. Hess, *J. Appl. Phys.* **52**, 7409 (1981).
- <sup>14</sup>M. O. Aboelfotoh and J. P. Doyle, *Phys. Rev. B* **59**, 10823 (1999).
- <sup>15</sup>T. Wimbauer, B. K. Meyer, A. Hofstaetter, A. Scharmann, and H. Overhof, *Phys. Rev. B* **56**, 7384 (1997).